Use of Laplacian Eigenfunctions and Eigenvalues for Analyzing Data on a Domain of Complicated Shape

Naoki Saito[1]

Department of Mathematics
University of California, Davis

May 23, 2007

[1] Partially supported by grants from National Science Foundation and Office of Naval Research. I thank Leo Chalupa (UCD, Neurobiology), Raphy Coifman (Yale), Julie Coombs (UCD, Neurobiology), Dave Donoho (Stanford), John Hunter (UCD), Peter Jones (Yale), Linh Lieu (UCD), Stan Osher (UCLA), Allen Xue (UCD), Katsu Yamatani (Meijo Univ.) for the fruitful discussions.

Outline

Outline

Motivations

- Consider a bounded domain of general (may be quite complicated) shape $\Omega \subset \mathbb{R}^d$.
- Want to analyze the spatial frequency information inside of the object defined in $\Omega \implies$ need to avoid the Gibbs phenomenon due to $\Gamma = \partial\Omega$.
- Want to represent the object information efficiently for analysis, interpretation, discrimination, etc. $\implies$ fast decaying expansion coefficients relative to a meaningful basis.
- Want to extract geometric information about the domain $\Omega \implies$ shape clustering/classification.

Motivations . . . Data Analysis on a Complicated Domain

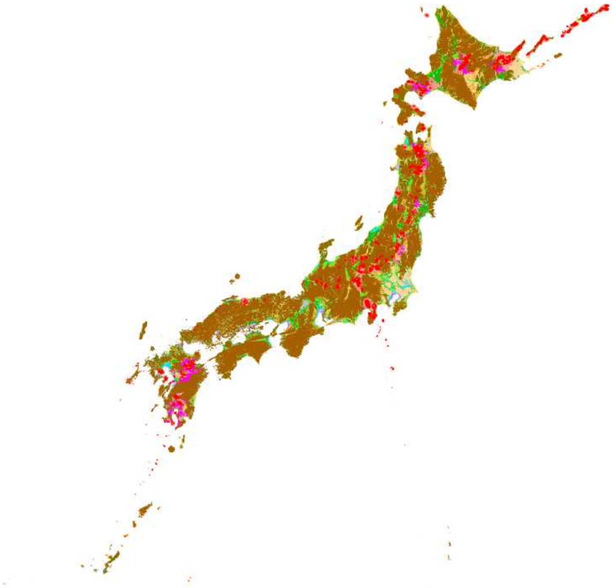

Motivations . . . Clustering Complicated Objects

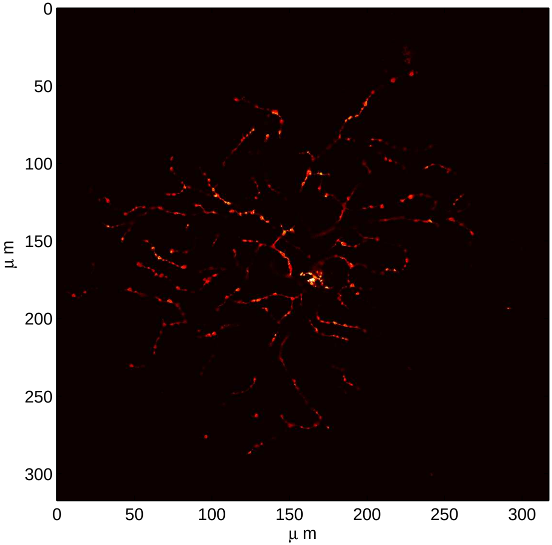

Motivations . . . Clustering Complicated Objects . . .

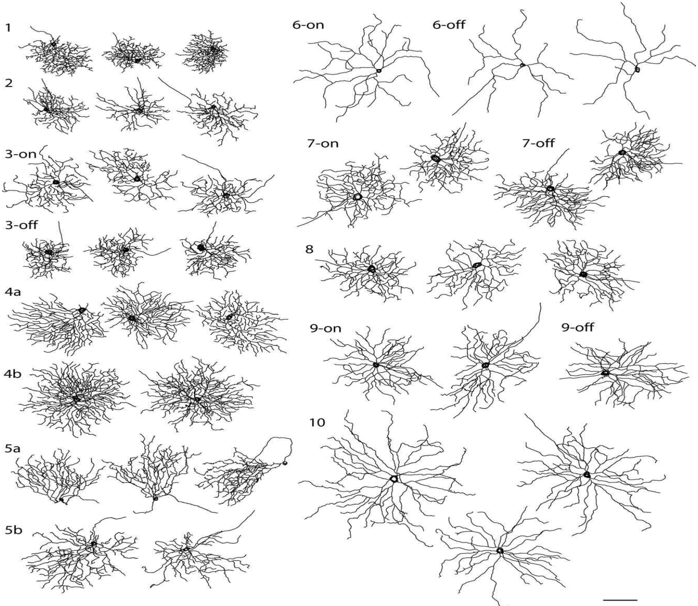

Outline

Eigenfunctions of Laplacian

- Our previous attempt was to extend the object to the outside smoothly and then bound it nicely with a rectangular box followed by the ordinary Fourier analysis.
- Why not analyze (and synthesize) the object using genuine basis functions tailored to the domain?
- After all, *sines* (and *cosines*) are the eigenfunctions of the Laplacian on the *rectangular* domain with Dirichlet (and Neumann) boundary condition.
- *Spherical harmonics, Bessel functions, and Prolate Spheroidal Wave Functions*, are part of the eigenfunctions of the Laplacian (via separation of variables) for the *spherical, cylindrical, and spheroidal* domains, respectively.

Eigenfunctions of Laplacian . . .

- Consider an operator $\mathcal{L} = -\Delta$ in $L^2(\Omega)$ with *appropriate* boundary condition.
- Analysis of $\mathcal{L}$ is difficult due to unboundedness, etc.
- Much better to analyze its inverse, i.e., the Green's operator because it is compact and self-adjoint.
- Thus $\mathcal{L}^{-1}$ has discrete spectra (i.e., a countable number of eigenvalues with finite multiplicity) except 0 spectrum.
- $\mathcal{L}$ has a complete orthonormal basis of $L^2(\Omega)$, and this allows us to do eigenfunction expansion in $L^2(\Omega)$.

Eigenfunctions of Laplacian . . . Difficulties

- The key difficulty is to compute such eigenfunctions; directly solving the Helmholtz equation (or eigenvalue problem) on a general domain is tough.
- Unfortunately, computing the Green's function for a general Ω satisfying the usual boundary condition (i.e., Dirichlet, Neumann) is also very difficult.

Outline

Integral Operators Commuting with Laplacian

- The key idea is to find an integral operator commuting with the Laplacian without imposing the strict boundary condition a priori.
- Then, we know that the eigenfunctions of the Laplacian is the same as those of the integral operator, which is easier to deal with, due to the following

Theorem (G. Frobenius 1878?; B. Friedman 1956)

Suppose $\mathcal{K}$ and $\mathcal{L}$ commute and one of them has an eigenvalue with finite multiplicity. Then, $\mathcal{K}$ and $\mathcal{L}$ share the same eigenfunction corresponding to that eigenvalue. That is, $\mathcal{L}\varphi = \lambda\varphi$ and $\mathcal{K}\varphi = \mu\varphi$.

Integral Operators Commuting with Laplacian ...

- Let's replace the Green's function $G(\mathbf{x}, \mathbf{y})$ by the fundamental solution of the Laplacian:

$$K(\mathbf{x}, \mathbf{y}) = \begin{cases} -\frac{1}{2}|x - y| & \text{if } d = 1, \\ -\frac{1}{2\pi} \log |\mathbf{x} - \mathbf{y}| & \text{if } d = 2, \\ \frac{|\mathbf{x}-\mathbf{y}|^{2-d}}{(d-2)\omega_d} & \text{if } d > 2. \end{cases}$$

- The price we pay is to have rather implicit, non-local boundary condition although we do not have to deal with this condition directly.

Integral Operators Commuting with Laplacian ...

- Let $\mathcal{K}$ be the integral operator with its kernel $K(\mathbf{x}, \mathbf{y})$:

$$\mathcal{K}f(\mathbf{x}) \triangleq \int_\Omega K(\mathbf{x}, \mathbf{y}) f(\mathbf{y}) \, \mathrm{d}\mathbf{y}, \quad f \in L^2(\Omega).$$

Theorem (NS 2005)

The integral operator $\mathcal{K}$ commutes with the Laplacian $\mathcal{L} = -\Delta$ with the following non-local boundary condition:

$$\int_\Gamma K(\mathbf{x}, \mathbf{y}) \frac{\partial \varphi}{\partial \nu_{\mathbf{y}}}(\mathbf{y}) \, \mathrm{d}s(\mathbf{y}) = -\frac{1}{2}\varphi(\mathbf{x}) + \ \mathrm{pv}\int_\Gamma \frac{\partial K(\mathbf{x}, \mathbf{y})}{\partial \nu_{\mathbf{y}}} \varphi(\mathbf{y}) \, \mathrm{d}s(\mathbf{y}),$$

for all $\mathbf{x} \in \Gamma$, where φ is an eigenfunction common for both operators.

Integral Operators Commuting with Laplacian . . .

Corollary (NS 2005)

The integral operator $\mathcal{K}$ is compact and self-adjoint on $L^2(\Omega)$. Thus, the kernel $K(\mathbf{x}, \mathbf{y})$ has the following eigenfunction expansion (in the sense of mean convergence):

$$K(\mathbf{x}, \mathbf{y}) \sim \sum_{j=1}^{\infty} \mu_j \varphi_j(\mathbf{x}) \overline{\varphi_j(\mathbf{y})},$$

and $\{\varphi_j\}_j$ forms an orthonormal basis of $L^2(\Omega)$.

Outline

Outline

1D Example

- Consider the unit interval $\Omega = (0, 1)$.
- Then, our integral operator $\mathcal{K}$ with the kernel $K(x, y) = -|x - y|/2$ gives rise to the following eigenvalue problem:

$$-\varphi'' = \lambda\varphi, \quad x \in (0, 1);$$

$$\varphi(0) + \varphi(1) = -\varphi'(0) = \varphi'(1).$$

- The kernel $K(\mathbf{x}, \mathbf{y})$ is of Toeplitz form $\Longrightarrow$ Eigenvectors must have even and odd symmetry (Cantoni-Butler '76).
- In this case, we have the following explicit solution.

1D Example . . .

- $\lambda_0 \approx -5.756915$, which is a solution of $\tanh \frac{\sqrt{-\lambda_0}}{2} = \frac{2}{\sqrt{-\lambda_0}}$,

$$\varphi_0(x) = A_0 \cosh \sqrt{-\lambda_0} \left(x - \frac{1}{2} \right);$$

- $\lambda_{2m-1} = (2m-1)^2\pi^2,\ m = 1, 2, \ldots,$

$$\varphi_{2m-1}(x) = \sqrt{2} \cos(2m-1)\pi x;$$

- $\lambda_{2m},\ m = 1, 2, \ldots$, which are solutions of $\tan \frac{\sqrt{\lambda_{2m}}}{2} = -\frac{2}{\sqrt{\lambda_{2m}}}$,

$$\varphi_{2m}(x) = A_{2m} \cos \sqrt{\lambda_{2m}} \left(x - \frac{1}{2} \right),$$

where $A_k,\ k = 0, 1, \ldots$ are normalization constants.

First 5 Basis Functions

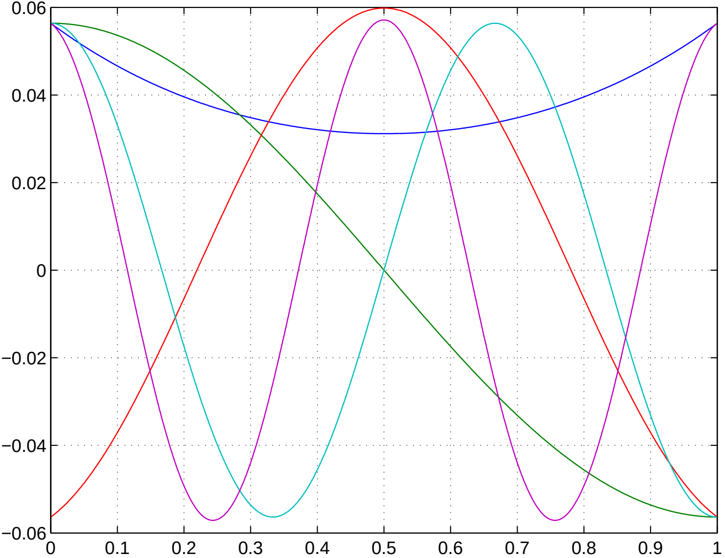

1D Example: Bases on Disconnected Intervals

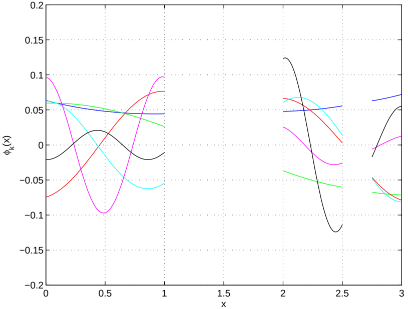

(a) Union

1D Example: Bases on Disconnected Intervals

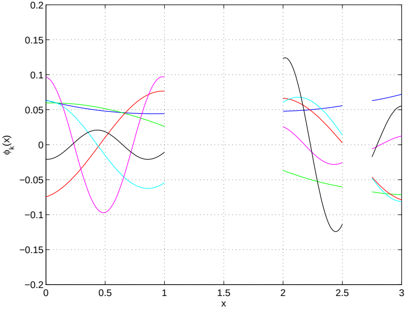

(a) Union

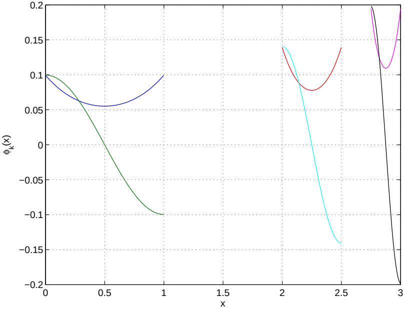

(b) Separated

Outline

2D Example

- Consider the unit disk Ω. Then, our integral operator $\mathcal{K}$ with the kernel $K(\mathbf{x}, \mathbf{y}) = -\frac{1}{2\pi} \log |\mathbf{x} - \mathbf{y}|$ gives rise to:

$$-\Delta\varphi = \lambda\varphi, \quad \text{in } \Omega;$$

$$\left.\frac{\partial\varphi}{\partial\nu}\right|_\Gamma = \left.\frac{\partial\varphi}{\partial r}\right|_\Gamma = -\left.\frac{\partial\mathcal{H}\varphi}{\partial\theta}\right|_\Gamma,$$

  where $\mathcal{H}$ is the Hilbert transform for the circle, i.e.,

$$\mathcal{H}f(\theta) \triangleq \frac{1}{2\pi}\ \mathrm{pv}\int_{-\pi}^{\pi} f(\eta) \cot\left(\frac{\theta-\eta}{2}\right) \mathrm{d}\eta \quad \theta \in [-\pi, \pi].$$

- Let $\beta_{k,\ell}$ is the ℓth zero of the Bessel function of order k, $J_k(\beta_{k,\ell}) = 0$. Then,

$$\varphi_{m,n}(r,\theta) = \begin{cases} J_m(\beta_{m-1,n}\, r)\binom{\cos}{\sin}(m\theta) & \text{if } m = 1, 2, \ldots,\ n = 1, 2, \ldots, \\ J_0(\beta_{0,n}\, r) & \text{if } m = 0,\ n = 1, 2, \ldots, \end{cases}$$

$$\lambda_{m,n} = \begin{cases} \beta^2_{m-1,n}, & \text{if } m = 1, \ldots,\ n = 1, 2, \ldots, \\ \beta^2_{0,n} & \text{if } m = 0,\ n = 1, 2, \ldots. \end{cases}$$

First 25 Basis Functions

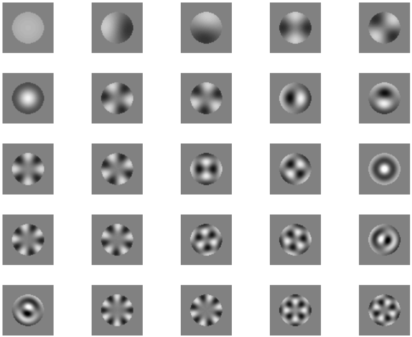

(a) Our Basis

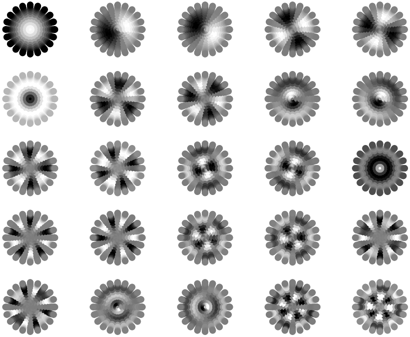

(b) Dirichlet-Laplace

Outline

3D Example

- Consider the unit ball Ω in $\mathbb{R}^3$. Then, our integral operator $\mathcal{K}$ with the kernel $K(\mathbf{x}, \mathbf{y}) = \frac{1}{4\pi|\mathbf{x}-\mathbf{y}|}$.
- Top 9 eigenfunctions cut at the equator viewed from the south:

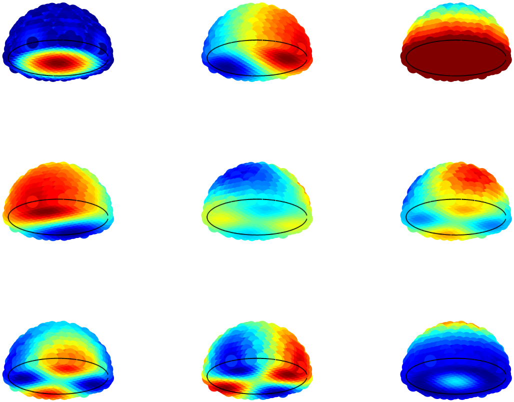

Outline

Discretization of the Problem

- Assume that the whole dataset consists of a collection of data sampled on a regular grid, and that each sampling cell is a box of size $\prod_{i=1}^{d} \Delta x_i$.
- Assume that an object of our interest Ω consists of a subset of these boxes whose centers are $\{\mathbf{x}_i\}_{i=1}^{N}$.
- Under these assumptions, we can approximate the integral eigenvalue problem $\mathcal{K}\varphi = \mu\varphi$ with a simple quadrature rule with node-weight pairs $(\mathbf{x}_j, w_j)$ as follows.

$$\sum_{j=1}^{N} w_j K(\mathbf{x}_i, \mathbf{x}_j)\varphi(\mathbf{x}_j) = \mu\varphi(\mathbf{x}_i), \quad i = 1, \ldots, N, \quad w_j = \prod_{i=1}^{d} \Delta x_i.$$

- Let $K_{i,j} \triangleq w_j K(\mathbf{x}_i, \mathbf{x}_j)$, $\varphi_i \triangleq \varphi(\mathbf{x}_i)$, and $\boldsymbol{\varphi} \triangleq (\varphi_1, \ldots, \varphi_N)^T \in \mathbb{R}^N$. Then, the above equation can be written in a matrix-vector format as: $K\boldsymbol{\varphi} = \mu\boldsymbol{\varphi}$, where $K = (K_{ij}) \in \mathbb{R}^{N \times N}$. Under our assumptions, the weight w_j does not depend on j, which makes K symmetric.

Outline

Outline

Image Approximation; Comparison with Wavelets

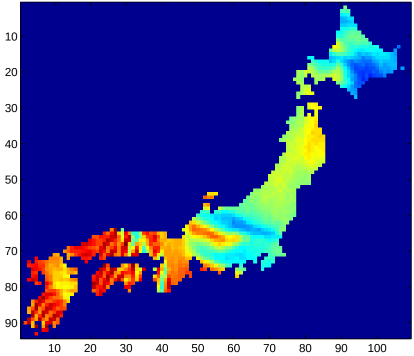

(a) What data?

Image Approximation; Comparison with Wavelets

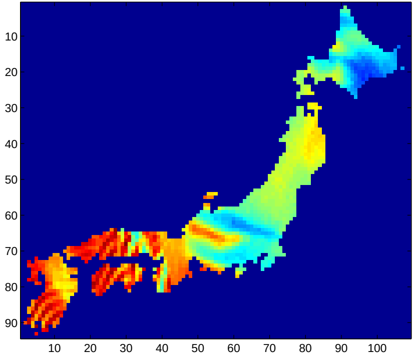

(a) What data?

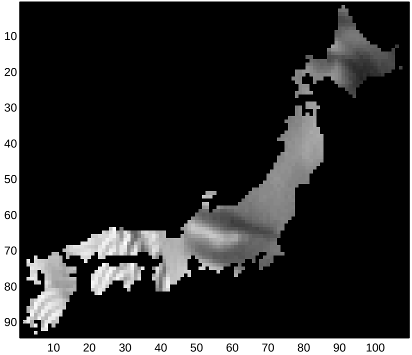

(b) $\chi_J \cdot$ Barbara

First 25 Basis Functions

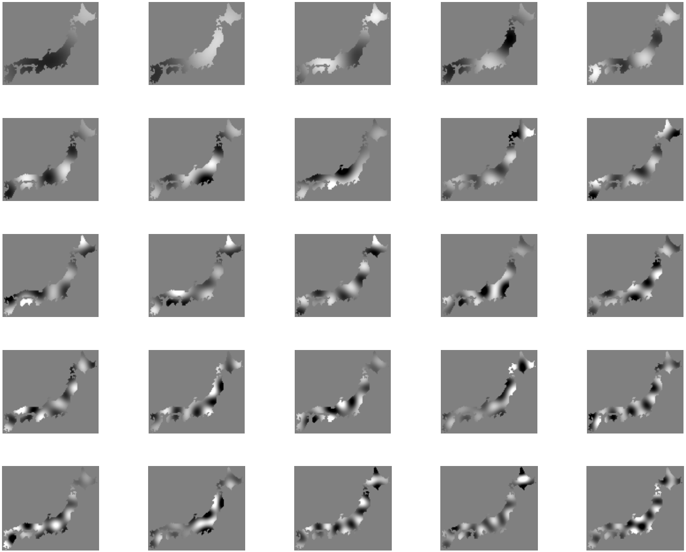

Next 25 Basis Functions

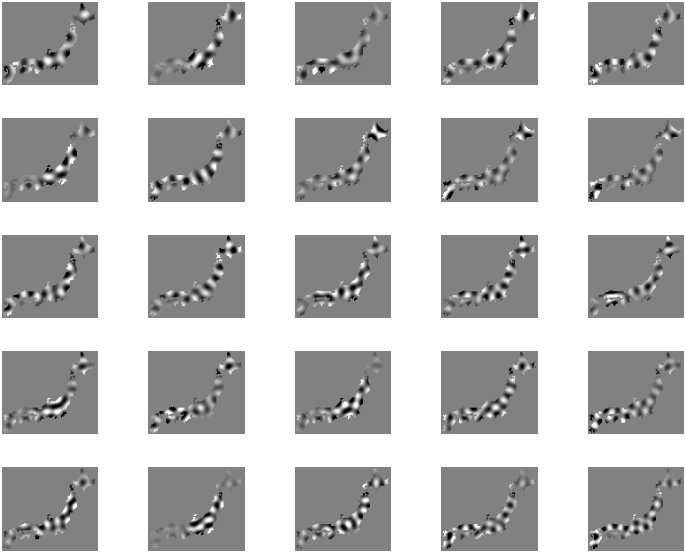

Reconstruction with Top 100 Coefficients

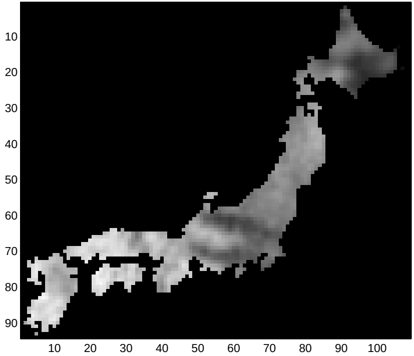

(a) Reconstruction

Reconstruction with Top 100 Coefficients

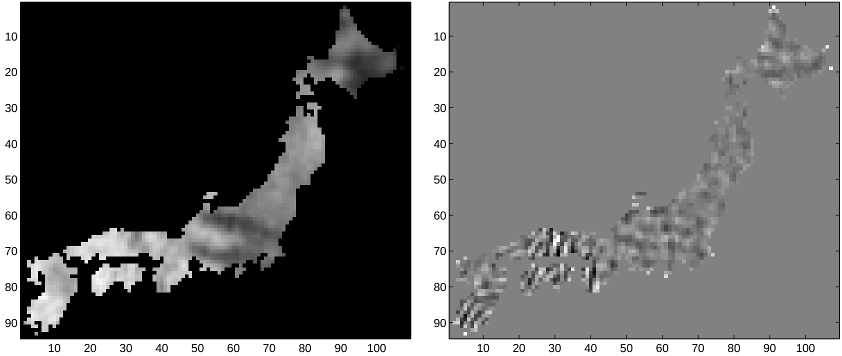

(a) Reconstruction (b) Error

Reconstruction with Top 100 2D Wavelets (Symmlet 8)

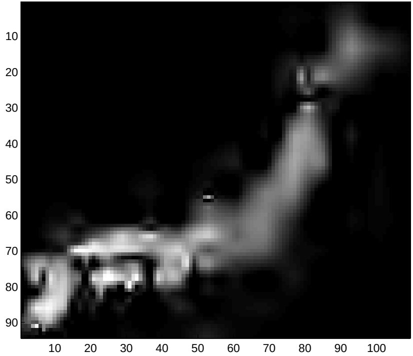

(a) Reconstruction

Reconstruction with Top 100 2D Wavelets (Symmlet 8)

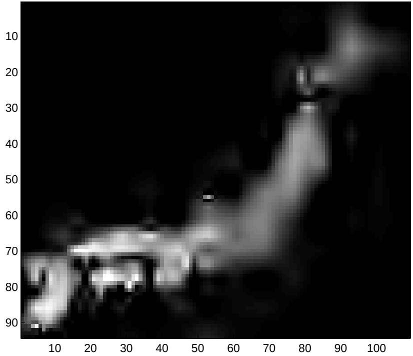

(a) Reconstruction

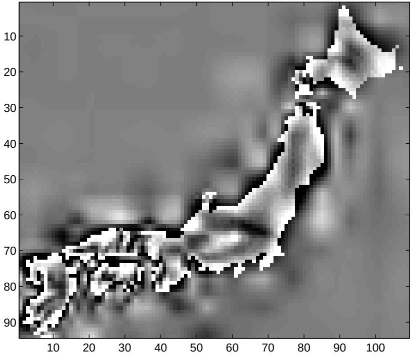

(b) Error

Reconstruction with Top 100 1D Wavelets (Symmlet 8)

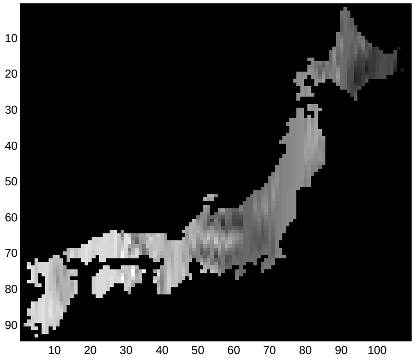

(a) Reconstruction

Reconstruction with Top 100 1D Wavelets (Symmlet 8)

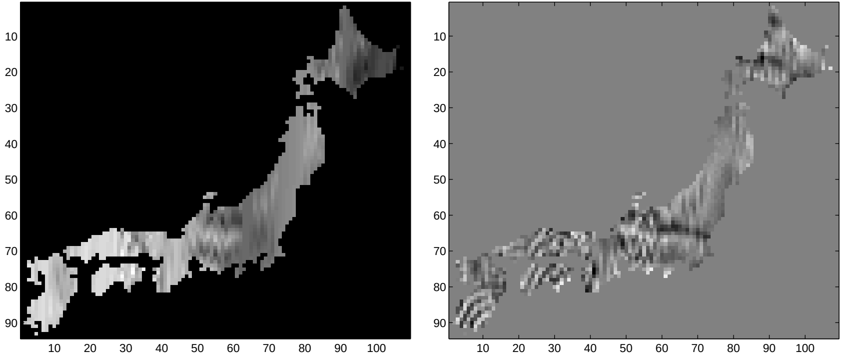

(a) Reconstruction (b) Error

Comparison of Coefficient Decay

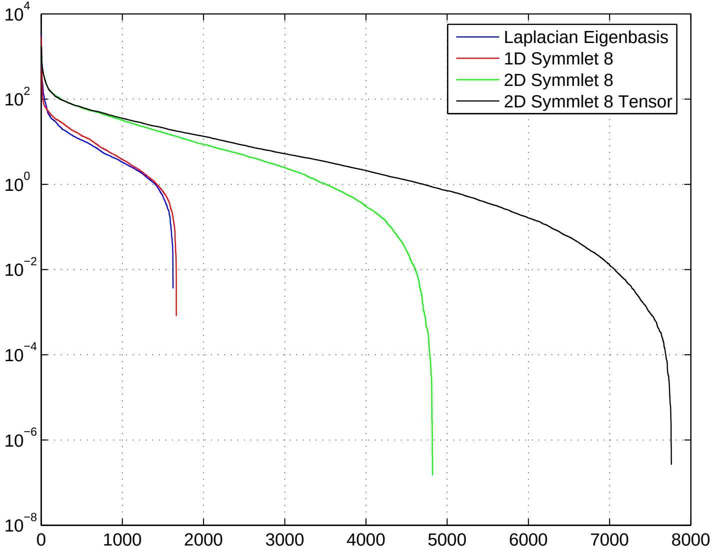

A Real Challenge: Kernel matrix is of 387924 × 387924.

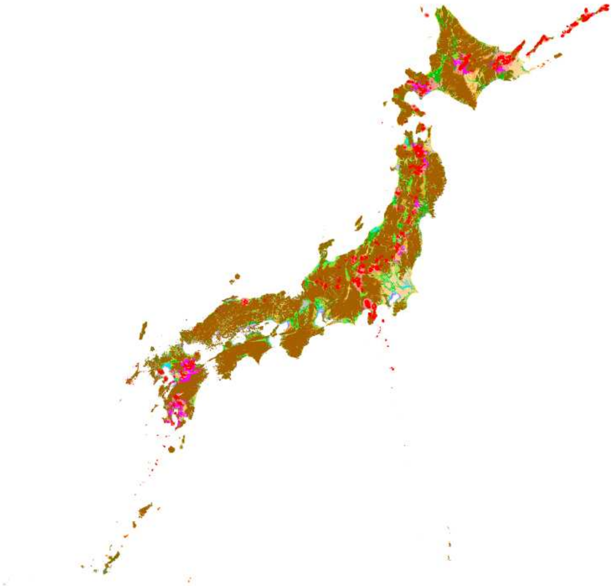

Conjecture on the Coefficient Decay Rate

Conjecture (NS 2005)

For $f \in C(\overline{\Omega})$ with $\nabla f \in BV(\overline{\Omega})$ defined on C^2-domain Ω, the expansion coefficients $\langle f, \varphi_k \rangle$ w.r.t. the Laplacian eigenbasis decay as $O(k^{-2})$. Thus, the N-term approximation error measured in the L^2-norm should have a decay rate of $O(N^{-1.5})$.

Outline

Comparison with PCA

- Consider a stochastic process living on a domain Ω.
- PCA/Karhunen-Loève Transform is often used.
- PCA/KLT incorporate geometric information of the measurement (or pixel) location through the data correlation, i.e., implicitly.
- Our Laplacian eigenfunctions use explicit geometric information through the harmonic kernel $\varphi(\mathbf{x}, \mathbf{y})$.

Comparison with PCA: Example

- *"Rogue's Gallery"* dataset from Larry Sirovich
- 72 training dataset; 71 test dataset
- Left & right eye regions

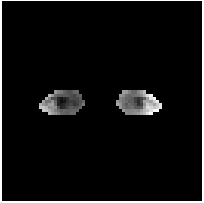
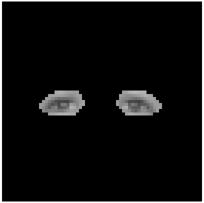
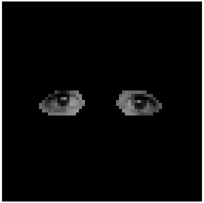

Comparison with PCA: Basis Vectors

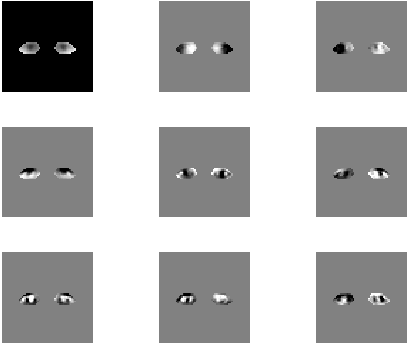

(a) KLB/PCA 1:9

Comparison with PCA: Basis Vectors

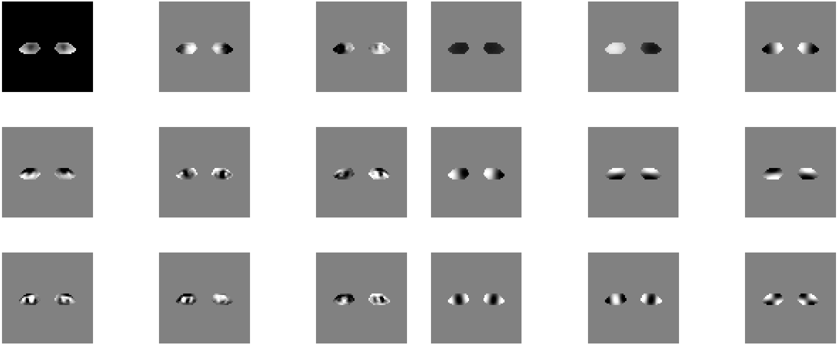

(a) KLB/PCA 1:9 (b) Laplacian Eigenfunctions 1:9

Comparison with PCA: Basis Vectors . . .

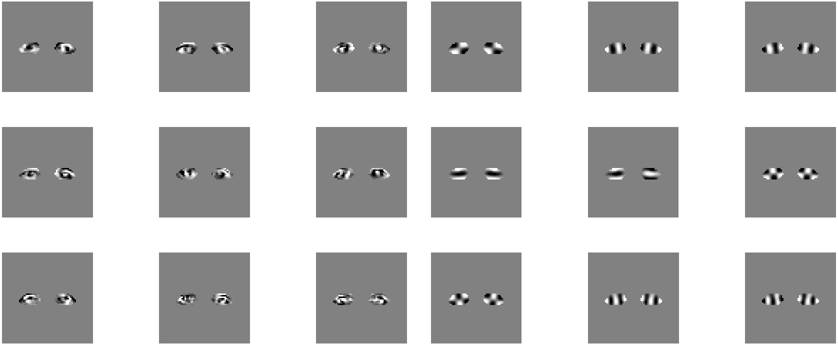

(a) KLB/PCA 10:18 (b) Laplacian Eigenfunctions 10:18

Comparison with PCA: Kernel Matrix

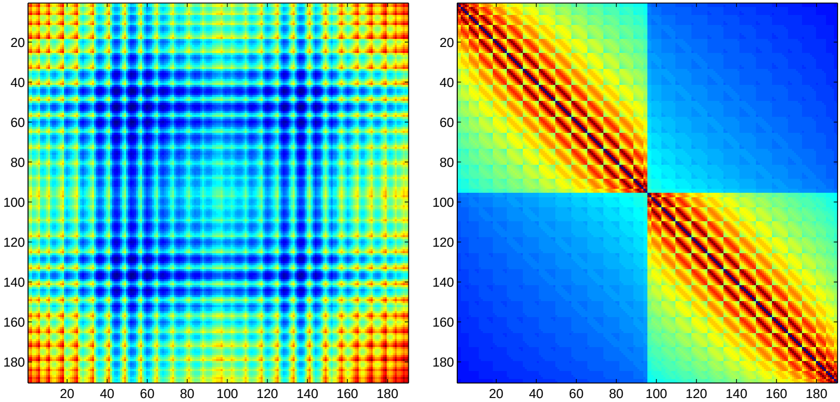

(a) Covariance (b) Harmonic kernel

Comparison with PCA: Energy Distribution over Coordinates

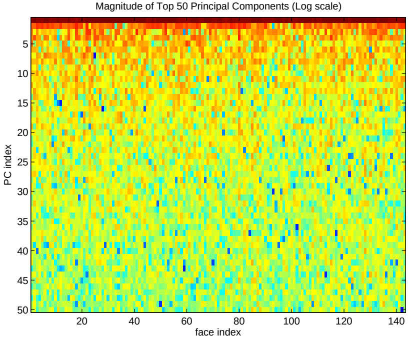

(a) KLB/PCA

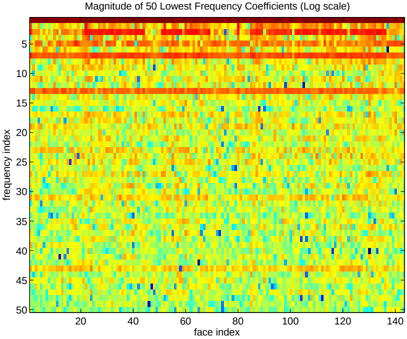

(b) Laplacian Eigenfunctions

Comparison with PCA: Basis Vector #7 . . .

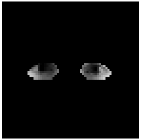

c_7:large

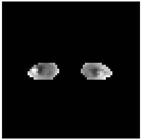

c_7:large

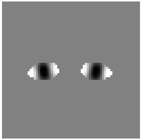

φ_7

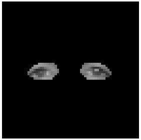

c_7:small

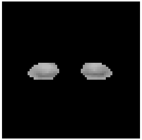

c_7:small

Comparison with PCA: Basis Vector #13 . . .

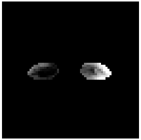

c_{13}:large

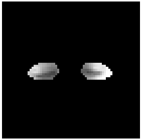

c_{13}:large

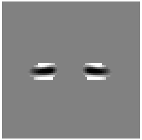

φ_{13}

c_{13}:small

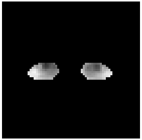

c_{13}:small

Outline

Solving the Heat Equation on a Complicated Domain

- It is well known that the semigroup $\mathrm{e}^{t\Delta}$ can be diagonalized using the Laplacian eigenbasis, i.e., for any initial heat distribution $u_0(\mathbf{x}) \in L^2(\overline{\Omega})$, we have the heat distribution at time t formally as

$$u(\mathbf{x}, t) = \mathrm{e}^{t\Delta} u_0 = \sum_{j=1}^{\infty} \mathrm{e}^{-t\lambda_j} \langle u_0, \varphi_j \rangle \varphi_j(\mathbf{x}),$$

which is based on the expansion of the Green's function for the heat equation $p_t(\mathbf{x}, \mathbf{y})$ via the Laplacian eigenfunctions as follows:

$$p_t(\mathbf{x}, \mathbf{y}) = \sum_{j=1}^{\infty} \mathrm{e}^{-\lambda_j t} \varphi_j(\mathbf{x}) \overline{\varphi_j(\mathbf{y})} \quad (t, \mathbf{x}, \mathbf{y}) \in (0, \infty) \times \overline{\Omega} \times \overline{\Omega}.$$

Solving the Heat Equation on a Complicated Domain

- Due to the discretization of the problem, we can write $\mathrm{e}^{t\Delta}$ in the matrix-vector notation as

$$\Phi\,\mathrm{e}^{-t\Lambda}\,\Phi^T = \Phi \text{ diag}\left(\mathrm{e}^{-t\lambda_1}, \ldots, \mathrm{e}^{-t\lambda_N}\right)\,\Phi^T = \sum_{j=1}^{N} \mathrm{e}^{-\lambda_j t} \varphi_j \varphi_j^T,$$

  where $\Phi = (\varphi_1, \ldots, \varphi_N)$ is the Laplacian eigenbasis matrix of size $N \times N$, and Λ is the diagonal matrix consisting of the eigenvalues of the Laplacian, which are the inverse of the eigenvalues of the kernel matrix, i.e., $\Lambda_{k,k} = \lambda_k = 1/\mu_k$.

- Given an initial heat distribution over the domain, $\mathbf{u}_0 \in \mathbb{R}^N$, we can compute the heat distribution at time t as

$$\mathbf{u}(t) = \Phi\,\mathrm{e}^{-t\Lambda}\,\Phi^T \mathbf{u}_0.$$

Solving the Heat Equation on a Complicated Domain . . .

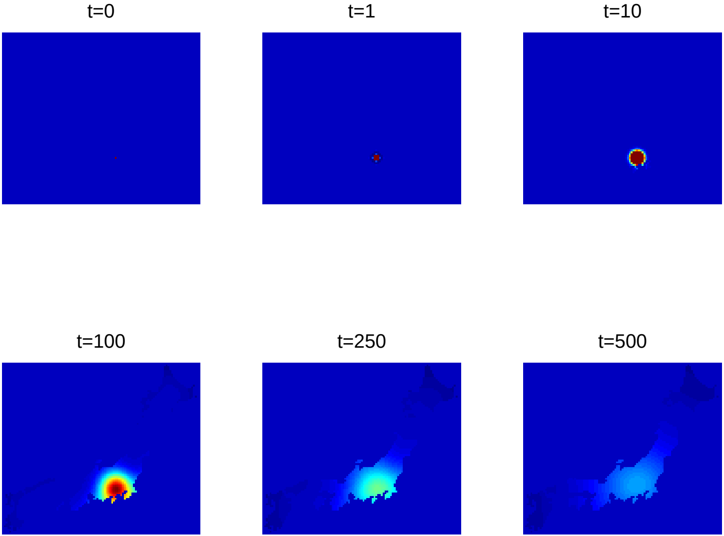

Solving the Heat Equation on a Complicated Domain . . .

- It is well known that the eigenvalues of the Laplacian with the Dirichlet (or the Neumann/Robin) boundary condition are positive (or non-negative).
- At this point, precisely specifying the boundary values is difficult because our formulation satisfies neither the Dirichlet nor the Neumann nor the Robin conditions.
- Our empirical observation so far has led to the following conjecture:

Conjecture (NS 2007)

The eigenvalues of the Laplacian satisfying our boundary condition and defined over a bounded domain $\Omega \in \mathbb{R}^d$ are all positive possibly with a finite number of negative ones.

Outline

Clustering Mouse Retinal Ganglion Cells

- Objective: To understand how the structural/geometric properties of mouse retinal ganglion cells (RGCs) relate to the cell types and their functionality
- Why mouse? $\Longrightarrow$ great possibilities for genetic manipulation
- Data: 3D images of dendrites/axons of RGCs
- State of the Art: Process each image via specialized software to extract geometric/morphological parameters (totally 14 such parameters) followed by a conventional clustering algorithm
- These parameters include: somal size; dendric field size; total dendrite length; branch order; mean internal branch length; branch angle; mean terminal branch length, etc. $\Longrightarrow$ takes half a day per cell with a lot of human interactions!

Clustering Mouse Retinal Ganglion Cells . . . 3D Data

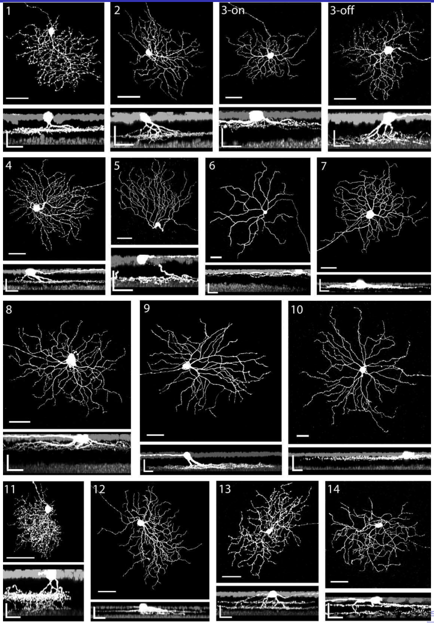

Very Preliminary Study on Mouse Retinal Ganglion Cells

- Use 2D plane projection data instead of full 3D
- Compute the smallest k Laplacian eigenvalues using our method (i.e., the largest k eigenvalues of $\mathcal{K}$) for each image
- Construct a feature vector per image
- Possible feature vectors reflecting geometric information: $\mathbf{F}_1 = (\lambda_1, \ldots, \lambda_k)^T$; $\mathbf{F}_2 = (\mu_1, \ldots, \mu_k)^T$; $\mathbf{F}_3 = (\lambda_1/\lambda_2, \ldots, \lambda_1/\lambda_k)^T$; $\mathbf{F}_4 = (\mu_1/\mu_2, \ldots, \mu_1/\mu_k)^T$.
- Do visualization and clustering

Very Preliminary Study on Mouse RGCs . . .

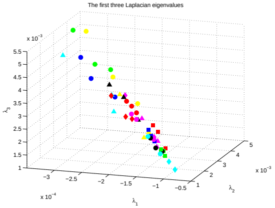

(a) $\mathbf{F}_1$

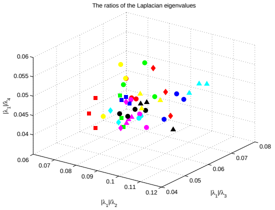

(b) $\mathbf{F}_3$

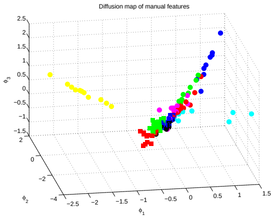

(c) *Manual*

Laplacian Eigenfunctions on a Mouse RGC

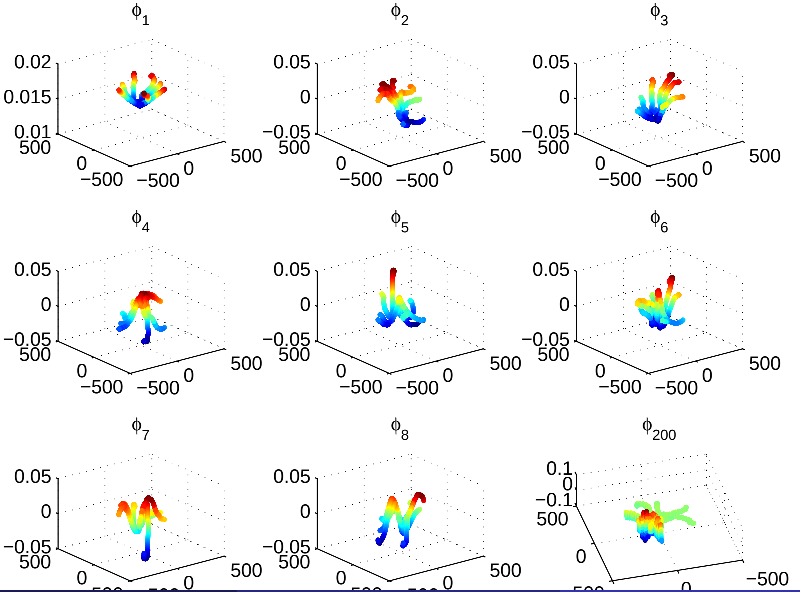

Challenges of Mouse Retinal Ganglion Cells

- Their shapes are very complicated.
- Interpretation of our eigenvalues are not yet fully understood compared to the usual Dirichlet-Laplacian case that have been well studied: the Payne-Pólya-Weinberger inequalities; the Faber-Krahn inequalities; the Ashbaugh-Benguria results, etc. For $\Omega \in \mathbb{R}^d$,

$$\lambda_1^{(D)}(\Omega) \geq \left(\frac{|\mathcal{B}_1^d|}{|\Omega|}\right)^2 \lambda_1^{(D)}(\mathcal{B}_1^d), \quad \frac{\lambda_{k+1}^{(D)}(\Omega)}{\lambda_k^{(D)}(\Omega)} \leq \frac{\lambda_2^{(D)}(\mathcal{B}_1^d)}{\lambda_1^{(D)}(\mathcal{B}_1^d)}, \quad k = 1, 2, 3.$$

  Note the related work on "Shape DNA" by Reuter et al. (2005), and classification of tree leaves by Khabou et al. (2007).
- Perhaps original 3D data should be used instead of projected 2D data.
- Reduce computational burden $\Longrightarrow$ need to develop fast algorithms.
- Heat propagation on the dendrites may give us interesting and useful information; after all the dendrites are network to disseminate information via chemical reaction-diffusion mechanism.
- Construct actual graphs based on the connectivity and analyze them directly via spectral graph theory and diffusion maps.

Outline

A Possible Fast Algorithm for Computing φ_j's

- Observation: our kernel function $K(\mathbf{x}, \mathbf{y})$ is of special form, i.e., the fundamental solution of Laplacian used in potential theory.
- Idea: Accelerate the matrix-vector product $K\varphi$ using the Fast Multipole Method (FMM).
- Convert the kernel matrix to the tree-structured matrix via the FMM whose submatrices are nicely organized in terms of their ranks. (Computational cost: our current implementation costs $O(N^2)$, but can achieve $O(N \log N)$ via the randomized SVD algorithm of Martinsson-Rokhlin-Tygert.)
- Construct $O(N)$ matrix-vector product module fully utilizing rank information (See also the work of Bremer (2007) and the "HSS" algorithm of Chandrasekaran et al. (2006)).
- Embed that matrix-vector product module in the Krylov subspace method, e.g., Lanczos iteration.
  (Computational cost: $O(N)$ for each eigenvalue/eigenvector).

Splitting into Subproblems for Faster Computation

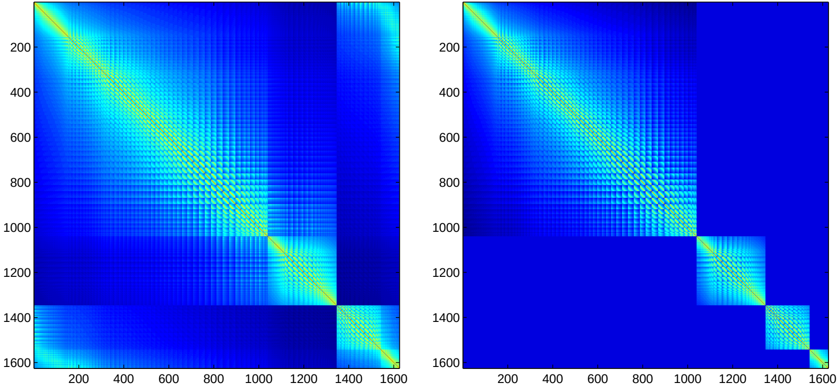

(a) Whole islands (b) Separated islands

Eigenfunctions for Separated Islands

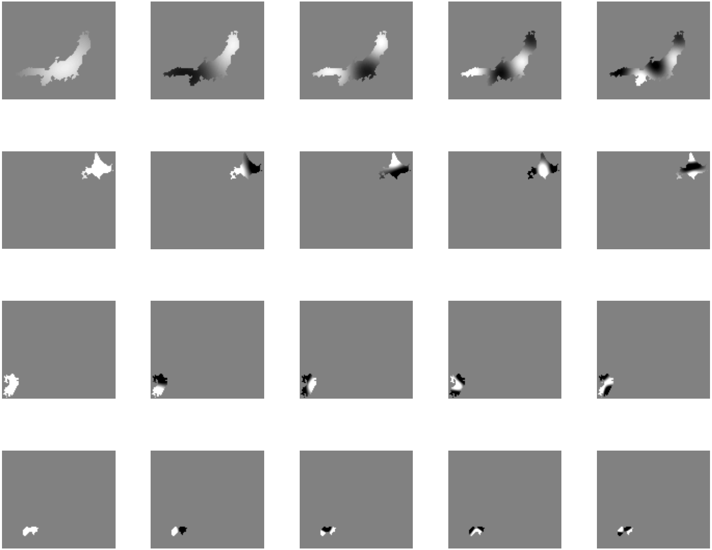

Outline

Conclusions

- Allow object-oriented image analysis & synthesis
- Can get fast-decaying expansion coefficients
- Can decouple geometry/domain information and statistics of data
- Can extract geometric information of a domain through the eigenvalues
- $\exists$ A variety of applications: interpolation, extrapolation, local feature computation, ...
- Fast algorithms are the key for higher dimensions/large domains
- Connection to lots of interesting mathematics: spectral geometry, spectral graph theory, isoperimetric inequalities, Toeplitz operators, PDEs, potential theory, almost-periodic functions, ...
- Many things to be done:
  - Synthesize the Dirichlet-Laplacian eigenvalues/eigenfunctions from our eigenvalues/eigenfunctions
  - How about higher order, i.e., polyharmonic ?
  - Features derived from heat kernels ?
  - Improve our fast algorithm

References

- The following articles are available at
  http://www.math.ucdavis.edu/~saito/publications/:

- N. Saito: "Geometric harmonics as a statistical image processing tool for images defined on irregularly-shaped domains," in *Proc. IEEE Workshop on Statistical Signal Processing*, Bordeaux, France, Jul. 2005.
- N. Saito: "Data analysis and representation using eigenfunctions of Laplacian on a general domain," Submitted to *Applied & Computational Harmonic Analysis*, Mar. 2007.

Thank you very much for your attention!